Journal of Physiology (1988), **403**, *pp.* 41–55
With 8 text-figures
Printed in Great Britain

OUTWARD RECTIFICATION OF INHIBITORY POSTSYNAPTIC CURRENTS IN CULTURED RAT HIPPOCAMPAL NEURONES

BY JEFFERY L. BARKER AND NEIL L. HARRISON*

From the Laboratory of Neurophysiology, NINCDS, National Institutes of Health 36/2C-02, Bethesda, MD 20892, U.S.A.

(*Received 12 May 1987*)

SUMMARY

1. Inhibitory postsynaptic potentials (IPSPs) and currents (IPSCs) were recorded from cultured hippocampal neurones of the embryonic rat at 22 °C, using the whole-cell patch-clamp technique with a low-Cl^-, 145 mM-potassium gluconate solution in the patch pipette. Individual synaptic events were elicited at low frequency (0·05–0·1 Hz) by stimulating a presynaptic neurone either by direct intracellular current injection, or by applying a brief pulse of L-glutamate.

2. In target neurones voltage clamped at −40 mV, outwardly directed IPSCs of mean amplitude 0·23 nA were recorded. The IPSCs were depressed by the GABA antagonist bicuculline, and reversed polarity between −50 and −80 mV (mean −64 mV), as did current responses to γ-aminobutyric acid. The IPSPs and IPSCs reversed as a single phase; no bicuculline-resistant 'late' synaptic event was observed.

3. The IPSCs had variable kinetics, with rise times between 1 and 5 ms (mean 2·9 ms) at −40 mV, and slower, monoexponential, decay phases (decay time constant, τ_{IPSC}, 10–40 ms at −40 mV). In some cells, τ_{IPSC} clearly increased with depolarization.

4. The IPSC reversal potential was -64 ± 9 mV ($n = 23$) under the experimental conditions used; this suggests that the synaptically activated channels are approximately 25 times more permeable to Cl^- than to the gluconate anion.

5. The peak conductance associated with the IPSC showed outward rectification. The synaptic conductance measured at −40 mV was 1·7 times greater than that measured at −100 mV; at −20 mV, synaptic conductance was 2·5 times greater than at −100 mV. This outward rectification can be explained by a constant field model under these experimental conditions of asymmetric Cl^- concentrations.

INTRODUCTION

γ-Aminobutyric acid (GABA) receptors coupled to Cl^- conductance mechanisms are widely distributed throughout vertebrate and invertebrate nervous systems. In crayfish or locust muscle (Dudel, 1977; Onodera & Takeuchi, 1979; Cull-Candy,

Authors are listed alphabetically.
* To whom correspondence should be addressed.

1984, 1986), and invertebrate neurones (Gardner, 1980*a*, *b*; Gardner & Stevens, 1980; Adams, Gage & Hamill, 1982; Adams, Banks & Constanti, 1981) the Cl^--dependent inhibitory postsynaptic current (IPSC) mediated by GABA or acetylcholine has been studied in detail. The GABA-mediated IPSCs have been studied in mammalian systems, using the hippocampal slice preparation (Collingridge, Gage & Robertson, 1984) or cultures of rat hippocampal neurones (Segal & Barker, 1984*b*). In both these studies, Cl^--filled microelectrodes were used to increase $[Cl^-]_i$ and thus shift the reversal potential for the IPSC in the depolarized direction. This permitted recordings of large-amplitude IPSCs at resting and more negative membrane potentials, but prevented study of the IPSC at more depolarized potentials. We have used the whole-cell patch clamp technique to study inhibitory synaptic transmission between cultured rat hippocampal neurones under conditions in which the cells are not loaded with Cl^- ions.

The results of our experiments demonstrate that postsynaptic depolarization over a physiologically relevant range of membrane potentials (-120 to -20 mV) results in intensification of the synaptically activated inhibitory conductance. Some of these observations have been the subject of a preliminary communication (Barker, Harrison & Vicini, 1986).

METHODS

Cell culture. Neurones from the hippocampi of E18 rat embryos were dissociated and maintained in dissociated culture for 2–5 weeks as previously described (Segal, 1983).

Electrophysiological recordings. Recordings were made at room temperature (19–24 °C) on the stage of an inverted phase-contrast microscope from neurones having cell bodies between 10 and 20 μm in diameter. The whole-cell variation of the patch clamp technique was used to record membrane currents or potentials (Hamill, Marty, Neher, Sakmann & Sigworth, 1981) via one or two List EPC-7 amplifiers. Pipette–membrane seals of 2–20 GΩ were necessary for successful recordings. Pipette-to-bath resistances prior to seal formation were 3–5 MΩ. Up to 70% series resistance compensation was obtained under voltage clamp.

Solutions. The patch pipettes were filled with an 'intracellular' solution containing (mM): potassium gluconate, 145; $MgCl_2$, 2; $CaCl_2$, 0·1; EGTA, 1·1; HEPES, 5; titrated to pH 7·2 with KOH. Sucrose was added to adjust the osmolarity to 315 mosM. Total intrapipette Cl^- was therefore 4·2 mM. The extracellular medium contained (mM): NaCl, 125; KCl, 5; $MgCl_2$, 8; $CaCl_2$, 4; D-glucose, 6; HEPES, 10; titrated to pH 7·4 with NaOH. Extracellular Cl^- was therefore 154 mM. The high level of Mg^{2+} in the extracellular medium was associated with a low level of spontaneous synaptic activity (Segal & Barker, 1984*b*). The liquid junction potential between the two solutions was eliminated by placing the reference electrode in a side compartment containing the 'intracellular' medium. The two compartments were connected with a bridge, filled on the reference electrode side with 'intracellular' medium and on the bath side with extracellular saline. An agar–saline 'plug' prevented mixing of the solutions, but ensured low (kΩ) electrical resistance.

Presynaptic stimulation. The postsynaptic events recorded were evoked either by direct injection of depolarizing current via a second 'intracellular' patch pipette (1 nA, 2–5 ms, 0·1 Hz), sufficient to trigger an action potential in the presynaptic neurone, or by stimulating another cell in the field of view with 50–100 ms pulses of L-glutamate, applied by pressure (1–2 lbf/in^2, 0·05–0·1 Hz) from a micropipette containing 20 μM-L-glutamate, placed close to the cell body of the 'presynaptic' neurone. The duration of the pressure pulse was adjusted until only one event was recorded per stimulus. The GABA and bicuculline were also applied by pressure from micropipettes placed within 2–3 μm of the 'postsynaptic' cell body.

Data aquisition and analysis. Pipette current or voltage was sampled and digitized at rates between 1 and 5 kHz, using a Data Translation analog-to-digital converter (12 bit, $\pm$5 V range).

Digitized data were stored for off-line analysis on a PDP 11–23 computer. Signals were low-pass filtered at half the sampling rate. The decay time constant, τ_{IPSC}, was estimated for individual currents (not averaged data) using a least-squares fitting routine. Synaptic latency was determined as the time elapsed between the peak of the presynaptic somatic action potential and the onset of the postsynaptic signal. Rise time was defined as the time taken for the IPSP or IPSC to grow from 10 to 90% of its peak amplitude. Where mean values of variables are given, these are quoted as mean ± standard deviation.

Calculation of peak synaptic conductance. The IPSC reversal potential, E_{IPSC}, was obtained by linear interpolation from the current–voltage relation for peak IPSC amplitude, I, for each target cell. The driving force for Cl^--ion movement, V_D, was then expressed for a given holding potential, V_H, as $V_D = V_H - E_{IPSC}$ (this assumes E_{IPSC} to be independent of V_H; see below and Fig. 6). The peak synaptic chord conductance was then defined as $g_{IPSC} = I/(V_H - E_{IPSC})$.

Fitting of experimental data by constant field model. In order to fit the experimental current–voltage relationships by a constant-field model, a modification of the Goldman–Hodgkin–Katz current equation (Hodgkin & Katz, 1949) was used to describe current flow by two permeant species through the synaptically activated ion channels. It was assumed that the only permeant ions were Cl^- and gluconate$^-$ (Gl^-); the permeability of gluconate through the channels was then defined as $P_{Gl} = k_{rel} P_{Cl}$, where k_{rel} is the ratio of permeabilities of gluconate relative to Cl^-. The equation used was:

$$i = \alpha V[([Cl^-]_o + k_{rel}[Gl^-]_o) - ([Cl^-]_i + k_{rel}[Gl^-]_i)\, e^{-VF/RT}],$$

where α is a constant inversely proportional to the absolute mobility of chloride ions, $[Cl^-]_o$ and $[Cl^-]_i$ are the external and internal concentrations of Cl^- ions, V is absolute membrane potential, and F,R, and T have their conventional meanings. The parameters α and k_{rel} were allowed to vary, using a non-linear least-squares algorithm, until a 'best fit' to the experimental data was obtained.

RESULTS

Cultured rat hippocampal neurones recorded from with patch pipettes containing potassium gluconate had resting membrane potentials between −50 and −60 mV, and input resistance between 100 and 500 MΩ. Injection of depolarizing current evoked one or more action potentials; prolonged current injection resulted in accommodation of firing. These electrophysiological properties are superficially similar to those reported for cultured hippocampal neurones impaled with conventional microelectrodes (Segal, 1983). Inhibitory synaptic connections were apparent after between 2–3 weeks in culture (Segal & Barker, 1984*b*). With gluconate as the main intracellular anion, and holding the membrane potential at −45 mV with injected depolarizing current, we could readily distinguish between hyperpolarizing inhibitory postsynaptic potentials (IPSPs) and depolarizing excitatory postsynaptic potentials (EPSPs); we studied only the IPSPs.

Properties of IPSPs

In eleven pairs of recorded neurones, IPSP latency was 3·4 ± 1·5 ms (range 1·2–5·5 ms). Synaptic latency varied little between stimuli (Fig. 1). Presynaptic firing rates up to 10 Hz were followed on a one-for-one basis by IPSPs in these synaptic pairs; such high-frequency stimulation of the presynaptic cell elicited the use-dependent depression of IPSPs previously described in rat hippocampal slices (McCarren & Alger, 1985). Often the presynaptic neurone failed to fire more rapidly than 10–20 Hz, perhaps due to mono- or polysynaptic feed-back inhibition mediated by recurrent collaterals of the presynaptic neurone itself. The IPSP rise time at −45 mV was 7·3 ± 3·2 ms (n = 11, range 3·6–14·5 ms). The IPSPs usually decayed in

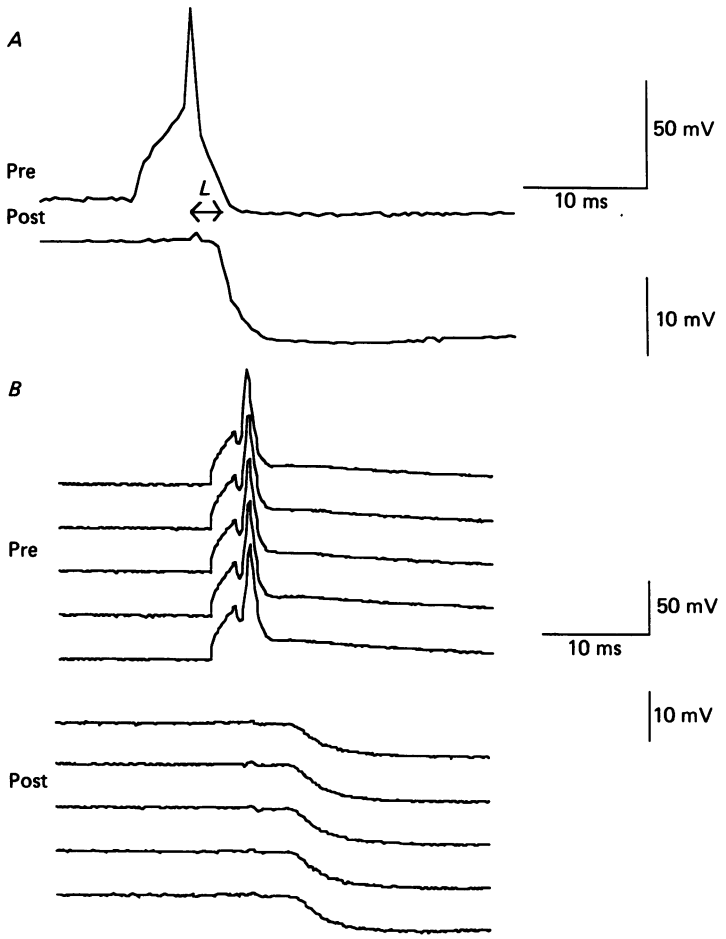

Fig. 1. Short latency monosynaptic IPSPs evoked by electrical stimulation of a presynaptic neurone. *A*, a single record shows an IPSP evoked by a single presynaptic action potential. The short synaptic latency is indicated (*L*). *B*, five consecutive records showing the stability of synaptic latency and IPSP amplitude.

a manner that could not be described by a single-exponential process (Dingledine & Korn, 1985); IPSP duration measured at half-peak amplitude was 73 ± 25 ms ($n = 11$, range 31–112 ms). They could be reversed in polarity between -60 and -70 mV by injection of hyperpolarizing current (Fig. 2*A*). The IPSPs reversed as a single phase with no evidence for a 'late' hyperpolarizing potential of the type described in adult rat hippocampal slices (Newberry & Nicoll, 1984*a*; Hablitz & Thalmann, 1987).

IPSPs and IPSCs reverse polarity at the reversal potential for current responses to GABA

Following identification of stable IPSPs in a postsynaptic cell, the neurone was voltage clamped at -40 mV. At this holding potential, presynaptic stimulation elicited outwardly directed IPSCs (mean amplitude 0·23 nA; range 0·04–0·82 nA).

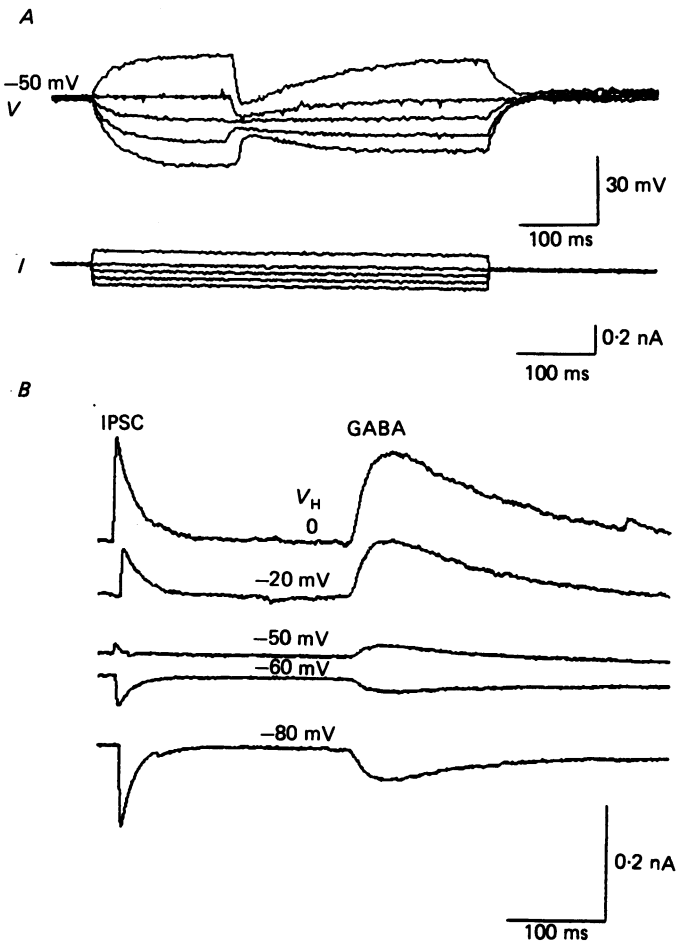

Fig. 2. IPSPs and IPSCs reverse polarity at E_{GABA}. *A*, IPSPs were evoked by L-glutamate stimulation of a presynaptic neurone. Injection of hyperpolarizing current at the postsynaptic cell body reverses the polarity of the evoked IPSP at about −60 mV. *B*, in another experiment, stimulation of the presynaptic neurone with L-glutamate was closely followed by application of a 15 ms pulse of 20 μM-GABA to the cell body of the voltage-clamped postsynaptic cell. It is apparent that the IPSC and current responses to exogenous GABA have a coincident reversal potential between −50 and −60 mV.

Between 20 and 500 IPSCs were recorded in each of thirty-two cells. In nine cells, reversal of the IPSC was not demonstrated convincingly, suggesting that the subsynaptic membrane was not under adequate voltage control; these data were discarded. In the remaining population of cells, the value of the reversal potential for the IPSC was -64 ± 9 mV (range −55 to −80 mV). In individual recordings, E_{IPSC} was identical with the reversal potential for current responses to GABA (E_{GABA}), evoked by 10–30 ms pulses at the cell body (Fig. 2*B*). This close correspondence between E_{IPSC} and E_{GABA} indicates that the ionic conductance activated by exogenous GABA and endogenous transmitter was identical. When 145 mM-KCl or CsCl replaced potassium gluconate in the patch pipette solution, both E_{IPSC} and

E_{GABA} shifted in the depolarizing direction, to between 0 and +5 mV. The IPSCs were reversibly depressed in amplitude by local application of the GABA antagonist bicuculline (not shown). Like the IPSPs and the current responses to GABA, IPSCs reversed as a single phase, with no evidence for a late, K^+-dependent synaptic current.

IPSC kinetics

In contrast to the complex decay of IPSPs, the vast majority of the IPSCs recorded in these experiments decayed as a single exponential at all membrane

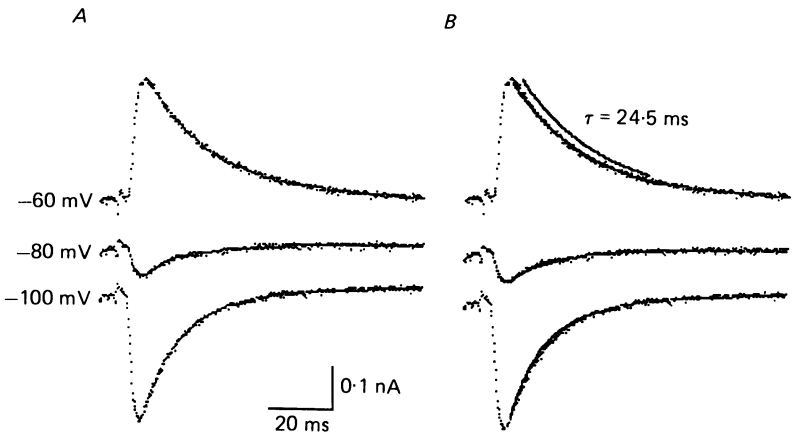

Fig. 3. IPSCs decay exponentially at all membrane potentials. *A*, raw data showing IPSCs recorded at holding potentials of −60, −80 and −100 mV in the same cell. *B*, the same data showing the exponential fit to the decay phase of the IPSC. All three IPSCs were very well fitted by a single-exponential decay phase. The fits to the IPSCs are superimposed on the original data; the fit to the first IPSC is also illustrated parallel to the fitted synaptic current. The IPSC decay time constant, τ_{IPSC} was 24·5, 15·7 and 10·4 ms respectively. Note that although τ_{IPSC} increases somewhat with depolarization in this case (see also Fig. 5), each IPSC still decays monoexponentially.

potentials studied (Fig. 3). A small proportion of IPSCs (< 10%) did not decay as a single exponential, having a 'tail' that was longer in duration than the majority of monoexponentially decaying IPSCs recorded. In view of the complexity of these events, our analysis is restricted to twenty-three cells in which IPSCs decayed with single-exponential kinetics. The IPSC rise time was estimated in thirteen cells; mean rise time was 2·9 ms (range 1·6–5·6 ms). The IPSC decay time measured at −40 mV varied considerably over twenty-three recordings; τ_{IPSC} was 27 ± 9 ms (range 11–41 ms). Over twenty-three recordings, τ_{IPSC} did not correlate with peak conductance (g_{IPSC}) (Fig. 4*A*; $P > 0{\cdot}1$, Kendall rank correlation test). In thirteen cells in which rise time and τ_{IPSC} were measured, there was a weak correlation between the two variables (Fig. 4*B*; $P < 0{\cdot}02$, Kendall rank correlation test). In eight cells, sufficient IPSCs were sampled to permit study of the voltage dependence of τ_{IPSC}; there was some increase in τ_{IPSC} with depolarization in five of the eight cells (e.g. Fig. 5*A*). In cells in which τ_{IPSC} increased with depolarization, there was no evidence that IPSC rise time was voltage dependent (Fig. 5*B*).

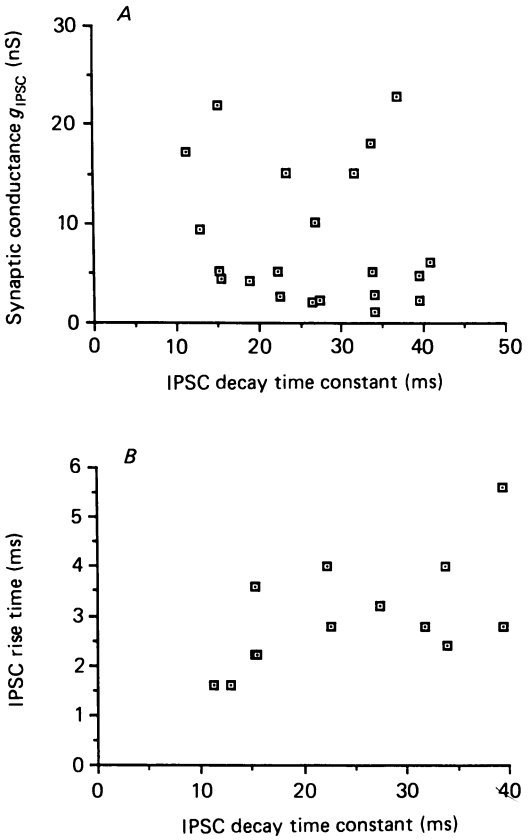

Fig. 4. τ_{IPSC} is weakly correlated with rise time but not with g_{IPSC}. *A*, the synaptic conductance g_{IPSC} associated with the IPSC recorded at −40 mV in each of twenty-one cells is plotted against the mean IPSC decay time constant τ_{IPSC} for IPSCs recorded at −40 mV in that cell. Each point represents the mean of 10–500 individual IPSCs. There was no correlation between the two variables. *B*, IPSC rise time is plotted against τ_{IPSC} for a population of thirteen cells in which IPSC rise time could be estimated accurately (in some cases the stimulus artifact arising from capacitative coupling between the two microelectrodes obscured the rising phase of the IPSC).

IPSCs show outward rectification

The amplitude of the IPSC varied in a non-linear manner with holding potential in most cells. In several experiments, the membrane potential was held at −40 mV, then the holding potential was changed to allow sampling of IPSCs at other membrane potentials for 30–90 s, before returning to −40 mV (method A). An example of a current–voltage relation obtained in this way is shown in Fig. 7*A*. In these initial experiments, it was assumed that E_{IPSC} is independent of holding potential; in other words it was assumed that conditioning the cell at various membrane potentials did not alter E_{Cl} and hence E_{IPSC}. This assumption was tested in a separate series of experiments in which the postsynaptic membrane was held at various potentials before being stepped to test potentials for 200 ms. The presynaptic cell was electrically stimulated 20 ms after the postsynaptic voltage jump was

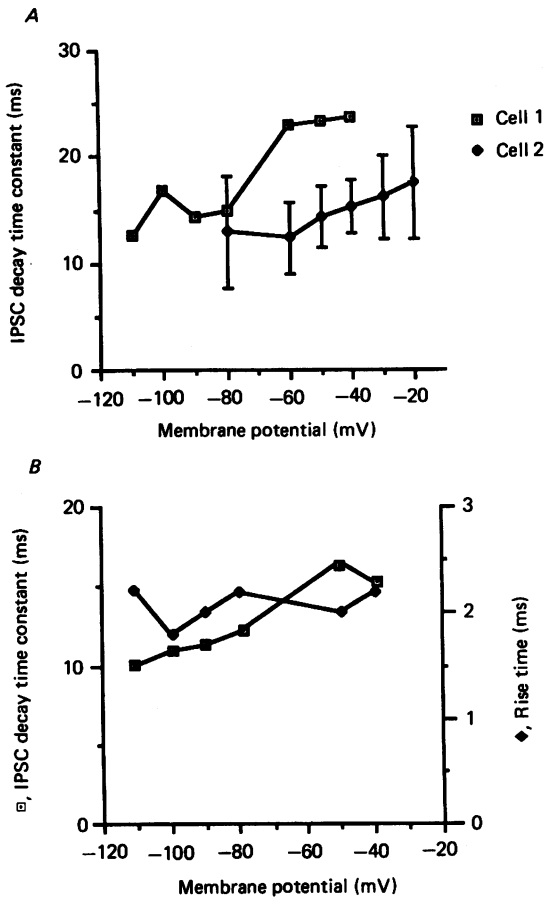

Fig. 5. IPSC decay time constant but not rise time is voltage dependent. *A*, IPSC decay time constant is plotted against holding potential for two different cells. Each point represents the mean decay time constant τ_{IPSC} for six to twenty-five IPSCs recorded at that holding potential. In one of the two experiments illustrated, a clear trend towards increased decay time constant is apparent with membrane depolarization. Error bars indicating standard deviation are shown for one cell only for clarity. *B*, voltage dependence of τ_{IPSC} but not rise time. In the example shown, τ_{IPSC} increases by $\sim 50\%$ between -110 and -20 mV, while rise time appears voltage invariant.

initiated (method B). In Fig. 6, it can be seen that conditioning the postsynaptic neurone for several minutes over a 40 mV range of holding potentials between -40 and -80 mV failed to influence the value of E_{IPSC}; this remained unchanged at -75 mV. This demonstration of the independence of E_{IPSC} from holding potential suggested that results obtained using the method A were valid, and the results of experiments using methods A and B were pooled.

By assuming E_{IPSC} to be invariant, it was possible to calculate synaptic conductance g_{IPSC} at a variety of holding potentials on either side of the reversal potential. Data from single cells transformed in this way also suggested outward rectification of the inhibitory conductance mechanism (Fig. 7*B*). When the

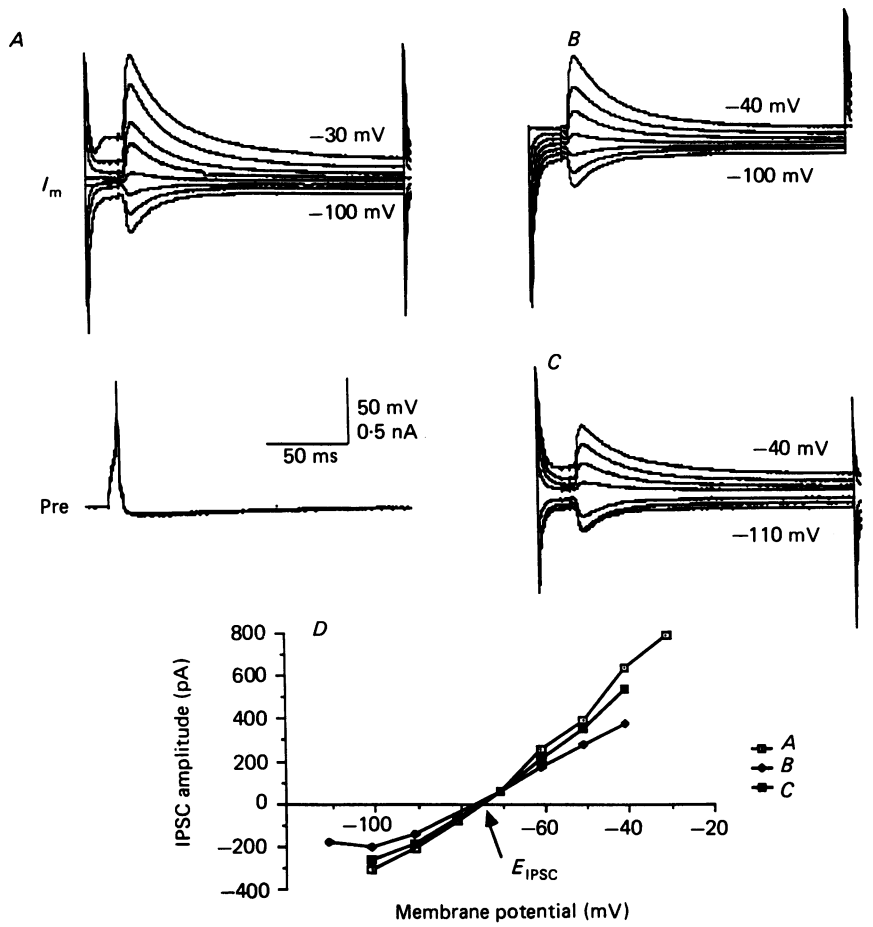

Fig. 6. The IPSC reversal potential E_{IPSC} is independent of holding potential under conditions of whole-cell recording. The membrane current (I_m) IPSCs recorded following voltage jumps from various holding potentials (V_H) to a series of test potentials. The postsynaptic cell was stepped from the holding potential to the test potential for 200 ms. Twenty milliseconds after the beginning of the step the presynaptic neurone (Pre) was electrically stimulated, firing a single action potential, which evokes an IPSC in the target cell. *A*, a family of synaptic currents recorded following voltage steps to test potentials between −30 and −100 mV, from a holding potential of −60 mV. The reversal potential for the IPSC, E_{IPSC}, was approximately −75 mV. Each current shown is an average of five to ten IPSCs obtained at each test potential. *B*, a family of synaptic currents recorded in the same cell by jumps to test potentials from −40 mV. The E_{IPSC} is again −75 mV. *C*, a family of synaptic currents recorded when the holding potential was −80 mV. The E_{IPSC} is −75 mV. *D*, current–voltage plots of the data for all three families of synaptic currents, showing identical reversal potentials and a modest degree of outward rectification.

population data were pooled, over a wide range of membrane potentials, the mean value of g_{IPSC} was 5·1 nS at −100 mV (twelve cells), 8·2 nS at −40 mV (twelve cells) and 9·2 nS at −20 mV (six cells).

Due to the intrinsic variability in synaptic conductance among recordings (range 1·2–23·0 nS at −40 mV), the statistical significance of the outward rectification was

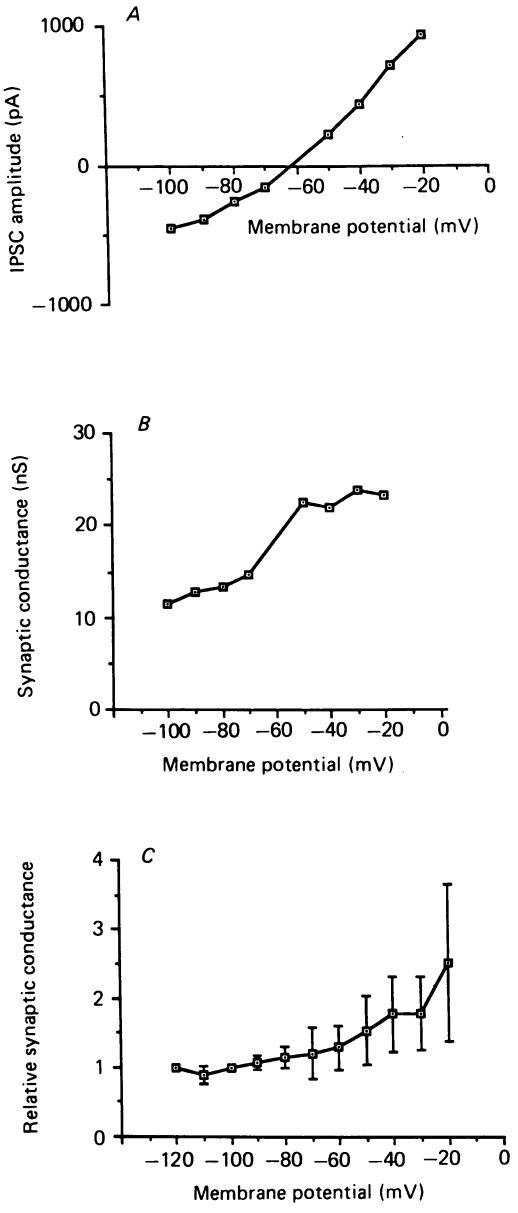

Fig. 7. Non-linearity of the inhibitory synaptic conductance. *A*, plot of IPSC peak amplitude measured at various holding potentials in a single cell, illustrating the non-linear nature of the current–voltage relationship. Each point represents the mean of five to thirty individual measurements at each potential. Variance was very small; standard deviations were less than 10% of the mean, and error bars are therefore not shown. *B*, the same data as shown in *A* are plotted as synaptic conductance g_{IPSC}. *C*, data from twelve cells were expressed as synaptic conductance relative to that measured at −100 mV, and the data were pooled. Each point represents the mean relative synaptic conductance from three to twelve cells at each given holding potential, relative to that at −100 mV (= 1·0). Error bars indicate the standard deviation about the arithmetic mean.

tested by expressing g_{IPSC} at a depolarized potential (−40 mV) as a ratio of g_{IPSC} measured at a hyperpolarized potential (−100 mV) *in the same cell*. Using this method, a conductance ratio was calculated for each of twelve cells. The conductance ratio for the population of twelve cells was 1·73±0·57. This ratio is significantly different from 1 ($P < 0{\cdot}001$, one-tailed t test). Conductance ratios relative to −100 mV were calculated for a wide range of membrane potentials (Fig. 7*C*),

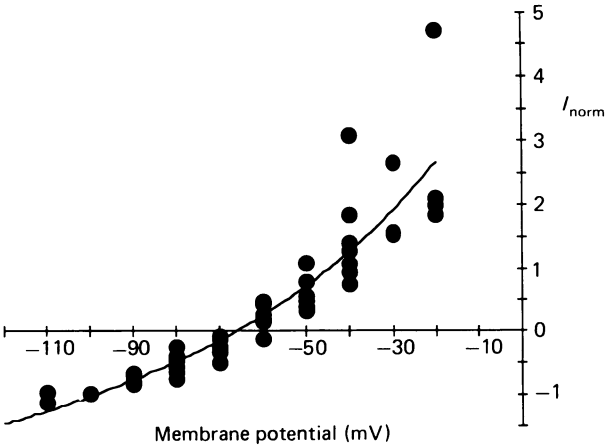

Fig. 8. Comparison of experimental rectification with Goldman rectification. Normalized current–voltage relation for pooled data from ten experiments, with currents (I_{norm}) expressed relative to synaptic current amplitude and sign at −100 mV, are shown together with the 'best-fit' predicted rectification based on the Goldman–Hodgkin–Katz equation. The 'best-fit' line estimates the IPSC reversal potential as −66 mV and the permeability ratio, k_{rel}, as 0·039.

indicating a trend toward outward rectification of the synaptic conductance at membrane potentials depolarized to the resting membrane potential. These experimental data can be compared with the predicted current–voltage curve calculated using the Goldman–Hodgkin–Katz current equation (Fig. 8). The pooled normalized data used in Fig. 7*C* were expressed as currents normalized to the current amplitude measured at −100 mV, and the resulting data were fitted using the constant field model (see Methods). The pooled data are well fitted by the Goldman–Hodgkin–Katz current equation, giving a best estimate of 0·0389 for k_{rel}, the permeability ratio (gluconate$^-$/Cl$^-$), and a 'best-fit' reversal potential of −66 mV. The approximation of the experimental data by the Goldman–Hodgkin–Katz equation is consistent with the explanation that the observed rectification of the IPSC arises from the asymmetric Cl$^-$ concentrations across the postsynaptic membrane.

DISCUSSION

We have studied inhibitory synapses between embryonic rat hippocampal neurones in dissociated culture. The coincident reversal potential for the IPSC and for GABA-evoked currents, the shift of IPSC reversal potential with high $[Cl^-]_i$ and the sensitivity of IPSCs to bicuculline all indicate that the IPSCs described here are Cl$^-$-dependent and mediated by GABA acting at the bicuculline-sensitive $GABA_A$

receptor (nomenclature from Hill & Bowery, 1981). No late K^+-dependent component of the synaptic signal was observed in these experiments. In addition, no *postsynaptic* response to the $GABA_B$ receptor agonist baclofen was obtained, although baclofen can reduce IPSC amplitude by a *presynaptic* action in cultured hippocampal neurones (Harrison, Lange & Barker, 1988). In preparations from the adult rat hippocampus, baclofen hyperpolarizes pyramidal neurones via an increase in K^+ conductance (Newberry & Nicoll, 1984*b*; Gahwiler & Brown, 1985). The absence of both *postsynaptic* baclofen responses and of the 'late' IPSP in our recordings is not inconsistent with the idea that these are generated by the same mechanisms.

Kinetics of IPSCs

Inhibitory postsynaptic potentials decayed with kinetics that could not be fitted with single-exponential models. However, almost all of the corresponding IPSCs recorded under voltage clamp decayed monoexponentially. This observation is consistent with previous recordings of IPSCs made with intracellular microelectrode techniques (Segal & Barker, 1984*b*; Collingridge *et al.* 1984). Exponential kinetics of synaptic current decay recorded at these and other types of chemical synapse have been interpreted as reflecting the probabilistic closure of ion channels opened as a consequence of postsynaptic receptor occupancy by the synaptic transmitter (Magleby & Stevens, 1972). The biphasic currents we occasionally observed may have arisen if significant numbers of synaptic endings invested electrotonically distant regions of the postsynaptic neurone, as well as regions close to and including the cell body (Nelson, Pun & Westbrook, 1986; see also Vicini, Wroblewski & Costa, 1986). The weak correlation between rise time and decay time constant observed in our recordings may be evidence for a more distant location of transmitter release sites in cases where both rise time and τ_{IPSC} are prolonged.

Amplitude of the IPSC

The evoked IPSC amplitudes reported here varied substantially over the population, most probably due to a large variability in the number of presynaptic release sites, but are of a similar order of magnitude to those reported by Collingridge *et al.* (1984) for spontaneous IPSCs in hippocampal slices. In both studies the recorded IPSCs reflect the activity of a single presynaptic neurone, and the size of the synaptic conductance increase is therefore many times less than that evoked by stimulation of inhibitory pathways in the hippocampal slice (Brown & Johnston, 1983), presumably because in the latter case multiple inhibitory units are activated.

Reversal potential and permeability ratio

In our recordings, the IPSC and GABA-evoked currents reversed polarity at -64 ± 9 mV. This is significantly more depolarized than predicted by the Nernst equation (−89 mV), assuming gluconate to be completely impermeant through the synaptically activated channels. Errors arising from incomplete compensation of series resistance were probably 2–3 mV at maximum. A similar value for E_{IPSP} is obtained with methanesulphonate replacing gluconate as anion (I. D. Forsythe & G. L. Westbrook, unpublished observations). The 'best-fit' curve obtained using the Goldman–Hodgkin–Katz current equation to fit the experimental data gave a

reversal potential of −66 mV, and the discrepancy between predicted and experimental reversal potentials can be explained if the gluconate anion permeability of the GABA-operated channel is approximately 0·04 times the Cl^- ion permeability.

Outward rectification of the IPSC

Under the recording conditions utilized here, the IPSC can be studied over a wide range of membrane potentials, revealing a modest but significant outward rectification of the peak synaptic conductance. Since the rise time of IPSCs is voltage-invariant in our recordings, we do not believe that the rectification of g_{IPSC} results from changes in the gating of synaptically activated channels with membrane depolarization. Furthermore, the rectification seems not to have arisen as a consequence of changes in E_{IPSC}, since E_{IPSC} proved rather insensitive to changes in holding potential (see Fig. 7). The values of E_{GABA} and E_{IPSC} certainly vary with membrane potential *in situ*, as observed with conventional microelectrode recordings (Ashwood, Collingridge, Herron & Wheal, 1987), but under conditions of whole-cell perfusion this appears not to be a factor in the interpretation of these synaptic conductance measurements.

Rectification of membrane current responses to exogenous GABA has been reported using potassium acetate microelectrodes in cultured hippocampal neurones (Segal & Barker, 1984*a*) and in the hippocampal slice (Ashwood *et al.* 1987). Single-channel recordings in membrane patches from cultured spinal neurones with asymmetric Cl^- concentrations also provide evidence for outward rectification (Hamill, Bormann & Sakmann, 1983). The present results show that this phenomenon extends to inhibitory synaptic currents at mammalian GABAergic synapses. Other Cl^--dependent synapses also show outward rectification (Dudel, 1977; Gardner, 1980*a*), and the rectification in each case may result from the asymmetric Cl^- concentrations across the postsynaptic membrane. The predicted current–voltage relation from the Goldman–Hodgkin–Katz equation provides a reasonably good fit to the experimental data (Fig. 8), and therefore suggests a parsimonious explanation for the observed macroscopic behaviour of the synaptic conductance.

Conclusion

Recordings of synaptic currents evoked by stimulation of presynaptic inhibitory neurones from embryonic rat hippocampus support the hypothesis that they are generated by a transient release of GABA, acting at $GABA_A$ receptors to stimulate an increase in Cl^- conductance. The synaptic current decays exponentially in a manner that is not incompatible with the probabilistic closure of individual ion channels. The IPSC decay time constant increases weakly, and peak synaptic conductance strongly, with membrane depolarization. The ability to make dual electrical recordings from pairs of synaptically coupled neurones should extend our understanding of this and other types of chemical synapse between central neurones grown in tissue culture.

We thank Veronica Smallwood for cultured hippocampal neurones, Dr Gerald Ehrenstein and Dr Paul Sheehy for help with curve fitting, and Dr G. David Lange and Dr Stefano Vicini for their participation in preliminary experiments.

REFERENCES

ADAMS, P. R., BANKS, F. W. & CONSTANTI, A. (1981). Voltage clamp analysis of inhibitory synaptic action in crayfish stretch receptor neurons. *Federation Proceedings* **40**, 2637–2641.

ADAMS, D. J., GAGE, P. W. & HAMILL, O. P. (1982). Inhibitory postsynaptic currents at *Aplysia* cholinergic synapses: effects of permeant anions and depressant drugs. *Proceedings of the Royal Society* B **214**, 335–350.

ASHWOOD, T. J., COLLINGRIDGE, G. L., HERRON, C. E. & WHEAL, H. V. (1987). Voltage-clamp analysis of somatic γ-aminobutyric acid responses in adult rat hippocampal CA1 neurones *in vitro*. *Journal of Physiology* **384**, 27–38.

BARKER, J. L., HARRISON, N. L. & VICINI, S. (1986). Non-linear behavior of the GABA-mediated inhibitory postsynaptic conductance in cultured rat hippocampal neurones. *Neuroscience Abstracts* **12**, 228.10.

BROWN, T. H. & JOHNSTON, D. (1983). Voltage-clamp analysis of mossy fiber synaptic input to hippocampal neurons. *Journal of Neurophysiology* **50**, 487–507.

COLLINGRIDGE, G. L., GAGE, P. W. & ROBERTSON, B. (1984). Inhibitory post-synaptic currents in rat hippocampal CA1 neurones. *Journal of Physiology* **356**, 551–564.

CULL-CANDY, S. G. (1984). Inhibitory synaptic currents in voltage-clamped locust muscle fibres desensitized to their excitatory transmitter. *Proceedings of the Royal Society* B **221**, 375–383.

CULL-CANDY, S. G. (1986). Miniature and evoked inhibitory junctional currents and γ-aminobutyric acid-activated current noise in locust muscle fibres. *Journal of Physiology* **374**, 179–200.

DINGLEDINE, R. & KORN, S. J. (1985). Gamma-aminobutyric acid uptake and the termination of inhibitory synaptic potentials in the rat hippocampal slice. *Journal of Physiology* **366**, 387–409.

DUDEL, J. (1977). Voltage dependence of amplitude and time course of inhibitory synaptic current in crayfish muscle. *Pflügers Archiv* **371**, 167–174.

GAHWILER, B. & BROWN, D. A. (1985). $GABA_B$ receptor-activated K^+ currents in voltage clamped CA3 pyramidal cells in hippocampal cultures. *Proceedings of the National Academy of Sciences of the U.S.A.* **82**, 1558–1562.

GARDNER, D. (1980*a*). Membrane potential effects on an inhibitory post-synaptic conductance in *Aplysia* buccal ganglia. *Journal of Physiology* **304**, 165–180.

GARDNER, D. (1980*b*). Time integral of synaptic conductance. *Journal of Physiology* **304**, 165–180.

GARDNER, D. & STEVENS, C. F. (1980). Rate-limiting step of inhibitory post-synaptic current decay in *Aplysia* buccal ganglia. *Journal of Physiology* **304**, 145–164.

HABLITZ, J. J. & THALMANN, R. (1987). Conductance changes underlying a late synaptic hyperpolarization in hippocampal CA3 neurons. *Journal of Neurophysiology* **58**, 160–179.

HAMILL, O. P., BORMANN, J. & SAKMANN, B. (1983). Activation of multiple-conductance state chloride channels in spinal neurones by glycine and GABA. *Nature* **305**, 805–808.

HAMILL, O. P., MARTY, A., NEHER, E., SAKMANN, B. & SIGWORTH, F. (1981). Improved patch-clamp techniques for high resolution current recording from cells and cell-free membrane patches. *Pflügers Archiv* **391**, 85–100.

HARRISON, N. L., LANGE, G. D. & BARKER, J. L. (1988). Baclofen activates presynaptic $GABA_B$ receptors on GABAergic neurons from the embryonic rat hippocampus. *Neuroscience Letters* **85**, 105–109.

HILL, D. R. & BOWERY N. G. (1981). ^{3}H-baclofen and ^{3}H-GABA bind to bicuculline-insensitive $GABA_B$ sites in rat brain. *Nature* **290**, 149–152.

HODGKIN, A. L. & KATZ, B. (1949). The effect of sodium ions on the electrical activity of the giant axon of the squid. *Journal of Physiology* **108**, 35–77.

MAGLEBY, K. L. & STEVENS, C. F. (1972). A quantitative description of end-plate currents. *Journal of Physiology* **223**, 173–197.

MCCARREN, M. & ALGER, B. E. (1985). Use-dependent depression of IPSPs in rat hippocampal pyramidal cells *in vitro*. *Journal of Neurophysiology* **53**, 557–571.

NELSON, P. G., PUN, R. & WESTBROOK, G. L. (1986). Synaptic excitation in cultures of mouse spinal cord neurones: receptor pharmacology and behaviour of synaptic currents. *Journal of Physiology* **372**, 169–180.

NEWBERRY, N. R. & NICOLL, R. A. (1984*a*). A bicuculline-resistant inhibitory post-synaptic potential in rat hippocampal pyramidal cells *in vitro*. *Journal of Physiology* **348**, 239–254.

NEWBERRY, N. R. & NICOLL, R. A. (1984*b*). Direct hyperpolarizing action of baclofen on hippocampal pyramidal cells. *Nature* **308**, 450–452.

ONODERA, K. & TAKEUCHI, A. (1979). An analysis of the inhibitory postsynaptic current in the voltage-clamped crayfish muscle. *Journal of Physiology* **286**, 265–282.

SEGAL, M. (1983). Rat hippocampal neurons in culture: responses to electrical and chemical stimuli. *Journal of Neurophysiology* **50**, 1249–1264.

SEGAL, M. & BARKER, J. L. (1984*a*). Rat hippocampal neurons in culture: properties of GABA-activated Cl^- ion conductance. *Journal of Neurophysiology* **51**, 500–515.

SEGAL, M. & BARKER, J. L. (1984*b*). Rat hippocampal neurons in culture: voltage-clamp analysis of inhibitory synaptic connections. *Journal of Neurophysiology* **52**, 469–487.

VICINI, S., WROBLEWSKI, J. T. & COSTA, E. (1986). Pharmacological modulation of GABAergic transmission in cultured cerebellar neurons. *Neuropharmacology* **25**, 207–211.